Published in final edited form as:
J Biomech. 2008 November 14; 41(15): 3213–3218. doi:10.1016/j.jbiomech.2008.08.012.

Quantification of the mechanical behavior of carotid arteries from wild-type, dystrophin-deficient, and sarcoglycan-δ knockout mice

Rudolph L. Gleason[1], **Wendy W. Dye**[2], **Emily Wilson**[3], and **Jay D. Humphrey**[2]

1 *George W. Woodruff School of Mechanical Engineering, Wallace H. Coulter Department of Biomedical Engineering, and The Petite Institute for Bioengineering and Bioscience, Georgia Institute of Technology, Atlanta, GA*

2 *Department of Biomedical Engineering and M.E. DeBakey Institute, Texas A&M University, College Station, TX*

3 *Department of Systems Biology and Translational Medicine, Texas A&M Health Science Center, College Station, TX*

Abstract

As patients with muscular dystrophy live longer because of improved clinical care, they will become increasingly susceptible to many of the cardiovascular diseases that affect the general population. There is, therefore, a pressing need to better understand both the biology and the mechanics of the arterial wall in these patients. In this paper, we use nonlinear constitutive relations to model, for the first time, the biaxial mechanical behavior of carotid arteries from two common mouse models of muscular dystrophy (dystrophin deficient and sarcoglycan-delta null) and wild-type controls. It is shown that a structurally motivated four-fiber family stress-strain relation describes the passive behavior of all three genotypes better than does a commonly used phenomenological exponential model, and that a Rachev-Hayashi model describes the mechanical contribution of smooth muscle contraction under basal tone. Because structurally motivated constitutive relations can be extended easily to model adaptations to altered hemodynamics, results from this study represent an important step toward the ultimate goal of understanding better the mechanobiology and pathophysiology of arteries in muscular dystrophy.

Keywords

muscular dystrophy; vascular mechanics; constitutive relation; wall stress; compensatory adaptations

Introduction

The dystrophin-glycoprotein complex (DGC) is a transmembrane molecular bridge that links cytoskeletal F-actin with the extracellular matrix protein laminin-2 and localizes many signaling proteins within muscle cells, including vascular smooth muscle. Genetic defects that compromise the DGC have been implicated in muscular dystrophies - progressive muscle disorders characterized by skeletal muscle weakness and wasting that affect approximately

Corresponding Author: R.L. Gleason, Ph.D., Georgia Institute of Technology, 315 Ferst Drive, Atlanta, GA 30332, E-mail: rudy.gleason@me.gatech.edu, (404) 385-7218 – phone, (404) 385-1397 – fax.

250,000 people in the United States alone. Whereas defects of the DGC are well studied in skeletal muscle, less is known about the role of this complex in vascular smooth muscle. Because the DGC likely plays key roles in mediating mechano-sensitive biological responses, its potential importance in the control of vascular wall biology and mechanics warrants additional study.

Previously, we compared biaxial biomechanical and vasoreactive functional responses of common carotid arteries from wild-type, dystrophin-deficient (mdx), and sarcoglycan-δ null (sgcd−/−) mice (Dye et al., 2007). In this paper, we report constitutive relations and best-fit values of material parameters that describe these previously reported data under both basal smooth muscle tone (basal) and maximally-dilated (passive) conditions. Specifically, using a two-dimensional (2-D) theoretical framework, we evaluated a phenomenological model proposed by Chuong and Fung (1986) and a structurally motivated four-fiber family model proposed by Baek et al. (2007) as possible descriptors of the passive biomechanical responses, and we evaluated the model proposed by Rachev and Hayashi (1999) for active smooth muscle. We found that the four-fiber family model (with 8 parameters) provided a better fit to the passive mechanical data from each genotype than did the Chuong and Fung model (with 7 parameters) and that it also provided quantitative interpretations that were more consistent with the prior experimental findings. In addition, the model of Rachev and Hayashi provided a reasonable description of the mechanical contribution of basal smooth muscle tone for each genotype. Having structurally motivated constitutive relations for the biomechanical behavior of carotid arteries from wild-type and muscular dystrophy mouse models is an important first step toward modeling adaptive processes that are important to clinical care.

Methods

Theoretical Framework

Mouse carotid arteries are long, straight, nearly cylindrical vessels with few or no branches, which facilitates both in vitro experimentation and constitutive formulations. We modeled these arteries using a 2-D framework and thus considered mean values for the intramural stresses. Reasons for this were twofold. First, residual stresses in arteries tend to homogenize the transmural distribution of stress under physiologic conditions, thereby rendering mean values of stress as good estimates of transmural values. Second, murine carotid arteries have a deformed thickness-to-radius ratio of ~0.07 and consist of only two-to-three layers of smooth muscle cells (cf. ~40 layers for human carotid arteries). In a 2-D setting, it is assumed that $\sigma_{rr} \ll \sigma_{\theta\theta}$ and $\sigma_{rr} \ll \sigma_{zz}$, where σ_{rr}, $\sigma_{\theta\theta}$, and σ_{zz} are mean values of the radial, circumferential, and axial components of Cauchy stress. Mean values for $\sigma_{\theta\theta}$, and σ_{zz} can be calculated directly from experimental data as

$$\sigma_{\theta\theta}=\frac{Pa}{h} \text{ and } \sigma_{zz}=\frac{f}{\pi h(2a+h)}, \tag{1}$$

where P is the transmural pressure, a and h are the luminal radius and wall thickness in a loaded configuration, and $f = f_T + \pi a^2 P$ is the total axial force applied to the vessel; f_T is the force measured via an in-line transducer and $\pi a^2 P$ accounts for the end-cap force that arises during in vitro testing. Because of the assumption that $\sigma_{rr} \approx 0$, appropriate nonlinear constitutive relations for mean values of $\sigma_{\theta\theta}$, and σ_{zz} are

$$\sigma_{\theta\theta}=\lambda_\theta^2\frac{\partial W}{\partial E_{\Theta\Theta}}-\lambda_r^2\frac{\partial W}{\partial E_{RR}}+\sigma_{\theta\theta}^{act}\ \text{and}\ \sigma_{zz}=\lambda_z^2\frac{\partial W}{\partial E_{ZZ}}-\lambda_r^2\frac{\partial W}{\partial E_{RR}}, \tag{2}$$

where λ_i are mean in-plane stretch ratios ($i = r,\theta,z$), E_{AA} are mean principal components of the Green strain ($A = R,\Theta,Z$; no sum), which is defined in the reference configuration, W is the strain-energy function for passive behavior, and $\sigma_{\theta\theta}^{act}$ describes the active contractile response of smooth muscle. Combining equations (1) and (2), we obtain relations suitable for parameter estimation, namely

$$P=\frac{h}{a}\left[\lambda_\theta^2\frac{\partial W}{\partial E_{\Theta\Theta}}-\lambda_r^2\frac{\partial W}{\partial E_{RR}}+\sigma_{\theta\theta}^{act}\right], \tag{3}$$

and

$$f_T=\pi h(2a+h)\left[\lambda_z^2\frac{\partial W}{\partial E_{ZZ}}-\lambda_r^2\frac{\partial W}{\partial E_{RR}}\right]-\pi a^2P, \tag{4}$$

which relate the measurable applied loads on the left-hand side of each equation with geometric changes and the constitutive model on the right hand side.

Constitutive Relations

Consider two candidate strain-energy functions W for the passive behavior: one proposed by Chuong and Fung (1986) and a four-fiber family model proposed by Baek et al. (2007), which is a straightforward extension of the two-fiber family model of Holzapfel et al. (2000). The model of Chuong and Fung is

$$W=\frac{c}{2}(e^Q-1) \tag{5}$$

where $Q=c_1E_{\Theta\Theta}^2+c_2E_{ZZ}^2+c_3E_{RR}^2+2c_4E_{\Theta\Theta}E_{ZZ}+2c_5E_{ZZ}E_{RR}+2c_6E_{RR}E_{\Theta\Theta}$ and c and $c_{1–6}$ are material parameters. The four-fiber family model is

$$W=\frac{b_1}{2}(I_1-3)+\sum_{k=1,2,3,4}\frac{b_2^k}{4b_3^k}\left\{\exp\left[b_3^k\left((\lambda^k)^2-1\right)^2\right]-1\right\} \tag{6}$$

where b_1, b_2^k, and b_3^k are material parameters, with k denoting a fiber family, $I_1 = tr(\mathbf{C}) = C_{RR} + C_{\theta\theta} + C_{ZZ}$ is the first invariant of the right Cauchy-Green strain tensor $\mathbf{C}$, where principal components of $\mathbf{C}$ are related to those of $\mathbf{E}$ via $C_{AA} = 2E_{AA} - 1$, $\lambda^k=\sqrt{\mathbf{M}^k\cdot\mathbf{C}\mathbf{M}^k}$ is the stretch of the k^{th} fiber family, $\mathbf{M}^k=\sin(\alpha_o^k)\mathbf{e}_\theta+\cos(\alpha_o^k)\mathbf{e}_z$ is the unit vector along the k^{th} fiber direction in the reference configuration, and α_o^k is the associated angle between the axial and fiber directions. In general, $(\lambda^k)^2=C_{\Theta\Theta}\sin^2(\alpha_o^k)+2C_{\Theta Z}\sin(\alpha_o^k)\cos(\alpha_o^k)+C_{ZZ}\cos^2(\alpha_o^k)$, but $C_{\Theta Z} = 0$ for

inflation and extension tests. We considered four fiber families with $\alpha_o^1=0°$ (axial), $\alpha_o^2=90°$ (circumferential), and $\alpha_o^3=-\alpha_o^4=\alpha_o$ (diagonal), which was left as a variable to be determined along with seven material parameters (with $b_2^3=b_2^4$ and $b_3^3=b_3^4$ for the diagonal fibers).

In addition, consider one model for the active (contractile) response of the smooth muscle cells under basal tone. Following Rachev and Hayashi (1999), we let

$$\sigma_\theta^{act}=T_{act}\lambda_\theta^2\left[1-\left(\frac{\lambda_M-\lambda_\theta}{\lambda_M-\lambda_0}\right)^2\right] \tag{7}$$

where λ_M is the stretch at which the contraction is maximum, λ_0 is the stretch at which active force generation ceases, and T_{act} is a parameter associated with the degree of muscle activation, which may be correlated with the intracellular calcium concentration.

Parameter estimation

Biaxial data came from Dye et al. (2007) for both passive and basal-tone conditions. Briefly, these data resulted from cyclic inflation tests performed at three fixed axial stretches (λ_z = 1.65, 1.80, and 1.95) and cyclic extension tests performed at three fixed transmural pressures (P = 60, 100, 140 mmHg). P, f_T, outer diameter d, and loaded length l were monitored continuously over two to three cycles for each protocol. Also measured directly were the unloaded outer diameter D and unloaded axial length L. In addition, wall thickness was measured at multiple static configurations and a mean value for vessel volume $\overline{V}$ was used to calculate the luminal radius $a=\sqrt{b^2-\overline{V}/(\pi\ell)}$ and thickness $h=(b-a)$ during cyclic testing; here b is the loaded outer radius. Mean circumferential stretch was calculated as $\lambda_\theta=r_{mid}/R_{mid}$, where mid-wall radii $r_{mid}=(a+b)/2$ and $R_{mid}=(A+B)\,2$, with A and B the unloaded inner and outer radii, and axial stretch was calculated as $\lambda_z=l/L$.

Best-fit values of material parameters for the passive Chuong and Fung model (c and $c_{1–6}$) and the four-fiber family model (b_1, b_2^k,b_3^k, and α_0, where k = 1, 2, and 3 = 4) were determined via a multi-dimensional nonlinear regression, using the Nelder-Mead direct search method, that minimized the error e between measured values of P and f_T on the left-hand side of equations (3) and (4) and calculated values on the right-hand side of equations (3) and (4), given measured values of λ_θ and λ_z. Namely, we minimized the error function

$$e=\sqrt{\frac{\sum_n(P_{meas}-P_{model})^2}{\sum_n(P_{meas})^2}}+\sqrt{\frac{\sum_n(f_{meas}-f_{model})^2}{\sum_n(f_{meas})^2}} \tag{8}$$

using the *fminsearch* subroutine in MatLab 6.1. Data were taken between 0 and 160 mmHg at increments of 2 mmHg for the $P-d$ tests and from the stretch at zero axial force to λ_z = 1.95 for the $f-l$ tests; taken together, the three $P-d$ tests and three $f-l$ tests yielded n = 325 to 350 data points. A penalty method was employed to ensure non-negative values of all best-fit parameters.

Data collected at basal smooth muscle tone over these same loading scenarios were used to determine the additional parameters for the active contractile response (λ_M, λ_o, and T_{act}). For these estimations, parameters for the four-fiber family model determined from passive data

were used to calculate the passive contribution to stress in equations (3) and (4). The error function (8) was again minimized via nonlinear regression for experimental values during $P - d$ and $f - l$ tests for vessels having a basal smooth muscle tone.

Results

Biomechanical data and modeling results for representative wild-type, mdx, and sgcd−/− carotid arteries illustrate the goodness of fit for the two passive models as well as the active model (Figure 1). Associated best-fit values of the model parameters and minimized error values for each vessel within each genotype (n = 5 or 6) are provided in Tables 1, 2, and 3, respectively. As it can be seen, the four-fiber family model provided a better overall fit to data (i.e., lower value of e) than did the model of Chuong and Fung for each vessel tested. Notice, too, that fiber directions $\alpha_o^3 = -\alpha_o^4 = \alpha_o$, as determined via nonlinear regression, were significantly different in vessels from the mdx (at $p = 0.013$) and scgd−/− mice (at $p = 0.056$) compared to vessels from the wild-type mice (Table 2 and Figure 2).

Discussion

By linking the cytoskeleton of muscle cells to adjacent extracellular matrix, the dystrophin-glycoprotein complex (DGC) helps to distribute mechanical stresses on these cells so as to maintain structural integrity during contraction and relaxation (Petrof et al. 1993; Pasternak et al. 1995). Absence of DGC components can thus have important implications for arteries, which consist largely of an abundant extracellular matrix with embedded smooth muscle cells that are subjected to continually changing wall shear and intramural (primarily circumferential and axial) stresses. Indeed, an altered biomechanical function of the vasculature in individuals with muscular dystrophy likely contributes to the progression of skeletal muscle weakness and wasting as well as diverse diseases related to diminished blood flow to end organs (Loufrani et al. 2004; Ito et al. 2006).

Surprisingly few investigators have studied the effects of muscular dystrophies on vascular biology and mechanics. We (Dye et al. 2007) and one group from Paris (Loufrani et al. 2001, 2002, 2004) have shown, however, that passive biomechanical behavior and smooth muscle contractility of carotid arteries are not statistically different under normal hemodynamic conditions in male wild-type (C57BL/6J), mdx barrier AX6 (on a C57BL/10SnJ background), and sgcd−/− (on a C57BL/6J background) mice, noting that mdx mice lack the protein dystrophin. It appears, therefore, that carotid arteries compensate, at least in part, during development for the absence of dystrophin or sarcoglycan-delta such that gross responses to normal hemodynamics are not compromised (e.g., mean arterial pressure and pressure-diameter responses are the same in mdx and wild-type controls). Nevertheless, Loufrani et al. (2001) found that “absence of dystrophin was associated with a defect in signal transduction of [flow-induced wall] shear stress.” That is, overall responses to the exogenous vasodilators acetylcholine (endothelial-dependent) and sodium nitroprusside (endothelial-independent) were normal, but dilation in response to increased shear stress was only 50–60% of normal in mdx mice. Whereas these experiments were performed acutely in isolated perfused vessels, the general importance of shear-regulated remodeling in vivo in response to sustained alterations in flow (e.g., Rudic et al., 2000; Schiffers et al., 2000; Sullivan and Hoying, 2002) suggests that a compromised shear-regulated dilatory function would adversely affect chronic adaptations (i.e., arterial growth and remodeling) to increased flow (as in exercise regimes, which are important but difficult to optimize for muscular dystrophy patients). Indeed, similar compromised adaptations to increased pressure (e.g., as in exercise or hypertension) should be expected, particularly given the important coupling of flow- and pressure-induced growth and remodeling in arteries (Ueno et al., 2000; Dajnowiec and Langille, 2007).

Gleason et al. (2004) and Gleason and Humphrey (2004) recently proposed models of arterial growth and remodeling in special cases of sustained alterations of flow and pressure. Such models promise to increase our understanding of adaptive processes and ultimately to aid in the design of improved clinical interventions (Humphrey and Taylor, 2008). Essential to models of growth and remodeling, however, is knowledge of the constitutive behavior of individual constituents. Although it is not possible, at present, to infer separately the mechanical properties of elastin, fibrillar collagen, and smooth muscle (the primary contributors to wall mechanics) from traditional inflation-extension tests, combining a structurally motivated constitutive model for passive behavior with a model for active smooth muscle enables one to approximate such properties. For example, in contrast to the phenomenological model of Chuong and Fung, the four-fiber family model enables one to estimate contributions due to the elastin-dominated amorphous matrix (isotropic term in equation 6) and contributions due to multiple families of fibrillar collagen (anisotropic terms in equation 6). Indeed, Wicker et al. (2008) show that this four-fiber family model captures mean collagen fiber angles in basilar arteries (measured independently using nonlinear optical microscopy), and comparison of the present best-fit values for b_1 (on the order of 10^1) with those of Wicker and colleagues (on the order of 10^{-7}) showed that the four-fiber family model captured the greater contribution of elastin in the mouse carotid artery (~28% elastin by dry weight) compared to the rabbit basilar artery (~5% elastin). Finally, the best-fit value of T_{act} (Table 3) was on the order of 10 to 25 kPa, which is reasonable for basal tone (cf. Rachev and Hayashi, 1999). The present results reveal quantitatively (i.e., lower best-fit value of e) and qualitatively (i.e., greater similarity of material parameters across genotypes) that this structurally motivated model fit biaxial data from three genotypes as well as or better than did the phenomenological model, hence providing both a foundation and a motivation for pursuing related growth and remodeling models. Toward this end, it is interesting that the best-fit values of the mean collagen fiber angle were significantly less (at a $p \leq 0.06$) for the muscular dystrophy models than for the wild-type controls. Although there is a need to determine directly if such a structural difference exists, this was not possible from the available standard histological data (Dye et al., 2007). In other words, the present theoretical finding provides guidance for future experiments as it should. It is provocative to note, however, that the lower best-fit value of $\alpha_o^3 = -\alpha_o^4 = \alpha_o$ for the two muscular dystrophy models is consistent with the previously observed lower values of in vivo axial stretch (Dye et al., 2007), which in turn was thought to reflect the primary compensatory adaptation by the mdx and sgcd−/− carotids under normal hemodynamics.

In conclusion, much remains to be learned with regard to compensatory adaptations by arteries during development in genetic models of disease as well as how these vessels respond to sustained alterations in hemodynamic loads in maturity. We submit that computational models will play an important role in this endeavor, thus using microstructurally motivated constitutive relations herein to quantify, for the first time, the mechanical behavior of carotid arteries from two common mouse model of muscular dystrophy is an important step toward this ultimate goal.

Acknowledgments

This work was supported, in part, by grants from the Muscular Dystrophy Association (MDA 3681) and the NIH (HL-64372). We also gratefully acknowledge Dr. Kevin P. Campbell, HHMI at the University of Iowa for providing the sgcd−/− breeding pairs.

References

Baek S, Gleason RL, Rajagopal KR, Humphrey JD. Theory of small on large: Potential utility in computations of fluid-solid interactions in arteries. Comput Methods Appl Mech Engng 2007;196:3070–3078.

Chuong CJ, Fung YC. On residual stress in arteries. J Biomech Eng 1986;108:189–192. [PubMed: 3079517]

Dajnowiec D, Langille BL. Arterial adaptations to chronic changes in haemodynamic function: coupling vasomotor tone to structural remodeling. Clin Sci (London) 2007;113:15–23. [PubMed: 17536999]

Dye W, Gleason RL, Wilson E, Humphrey JD. Altered biomechanical properties of carotid arteries in two mouse models of muscular dystrophy. J Appl Physiol 2007;103:664–672. [PubMed: 17525297]

Gleason RL, Humphrey JD. A mixture model of arterial growth and remodeling in hypertension: altered muscle tone and tissue turnover. J Vasc Res 2004;41:352–363. [PubMed: 15353893]

Gleason RL, Taber LA, Humphrey JD. A 2-D model of flow-induced alterations in the geometry, structure, and properties of carotid arteries. J Biomech Eng 2004;126:371–381. [PubMed: 15341175]

Holzapfel GA, Gasser TC, Ogden RW. A new constitutive framework for arterial wall mechanics and a comparative study of material models. J Elast 2000;61:1–48.

Humphrey JD, Taylor CA. Intracranial and abdominal aortic aneurysms: Similarities, differences and need for a new class of computational models. Ann Rev Biomed Eng. 2008in press

Ito K, Kimura S, Ozasa S, Matsukura M, Ikezawa M, Yoshioka K, Ueno H, Suzuki M, Araki K, Yamamura K, Miwa T, Dickson G, Thomas G, T M. Smooth muscle-specific dystrophin expression improves aberrant vasoregulation in mdx mice. Human Molc Gen 2006;15:2266–2275.

Loufrani L, Dubroca C, You D, Levy B, Paulin D, Henrion D. Absence of dystrophin in mice reduces NO-dependent vascular function and vascular density: Total recovery after a treatment with the aminogylcoside gentamicin. Arterioscler Thromb Vasc Biol 2004;20:671–676. [PubMed: 14751810]

Loufrani L, Levy B, Henrion D. Defect in microvascular adaptation to chronic changes in blood flow in mice lacking the gene encoding for dystrophin. Circ Res 2002;91:1183–1189. [PubMed: 12480820]

Loufrani L, Matrougui K, Gorny D, Duriez M, Blanc I, Levy B, Henrion D. Flow (shear stress)–induced endothelium-dependent dilation is altered in mice lacking the gene encoding for dystrophin. Circulation 2001;103:864–870. [PubMed: 11171796]

Pasternak C, Wong S, Elson E. Mechanical function of dystrophin in muscle cells. J Cell Biol 1995;128:355–361. [PubMed: 7844149]

Petrof B, Shrager J, Stedman H, Kelly A, Sweeney H. Dystrophin protects the sarcolemma from stresses developed during muscle contraction. Proc Natl Acad Sci U S A 1993;90:3710–3714. [PubMed: 8475120]

Rachev A, Hayashi K. Theoretical study of the effects of vascular smooth muscle contraction on strain and stress distributions in arteries. Ann Biomed Eng 1999;27:459–468. [PubMed: 10468230]

Rudic RD, Bucci M, Fulton D, Segal SS, Sessa WC. Temporal events underlying arterial remodeling after chronic flow reduction in mice. Correlation of structural changes with a deficit in basal nitric oxide synthesis. Circ Res 2000;86:1160–1166. [PubMed: 10850968]

Schiffers P, Henrion D, Boulanger C, Colucci-Guyon E, Langa-Vuves F, van Essen H, Fazzi G, Levy B, De Mey J. Altered flow-induced arterial remodeling in vimentin-deficient mice. Arterioscler Thromb Vasc Biol 2000;20:611–616. [PubMed: 10712381]

Sullivan CJ, Hoying JB. Flow-dependent remodeling in the carotid artery of fibroblast growth factor-2 knockout mice. Arterioscler Thromb Vasc Biol 2002;22:1100–1105. [PubMed: 12117723]

Ueno H, Kanellakis P, Agrotis A, Bobik A. Blood flow regulates the development of vascular hypertrophy, smooth muscle cell proliferation, and endothelial cell nitric oxide synthase in hypertension. Hypertension 2000;36:89–96. [PubMed: 10904018]

Wicker B, Hutchens H, Wu Q, Yeh A, Humphrey J. Normal basilar artery structure and biaxial mechanical behavior. Comp Meth Biomech Biomed Engng. 2008in press

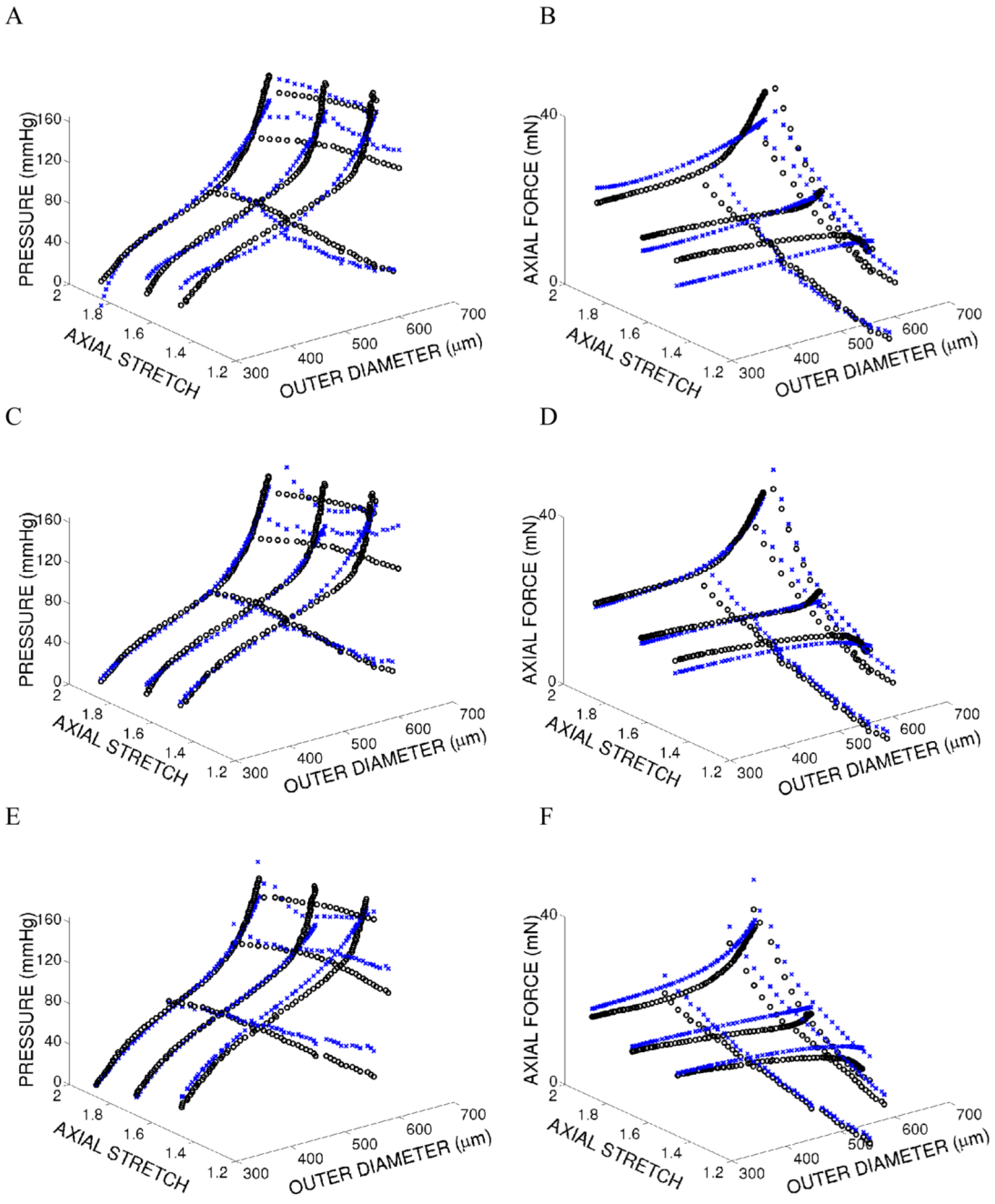

Figure 1.

Experimental data (open black circles) and model predictions (x's) for the final cycle of loading for three different fixed-length cyclic inflation and three different fixed-pressure cyclic extension tests for vessel MDX 020105. Panels A and B show passive biomechanical data and the fit of the Chuong and Fung model. Panels C and D show passive biomechanical data and the fit of the four-fiber family model. Panels E and F show biomechanical data under basal tone and the fit of the active model (using the passive four-fiber family model)

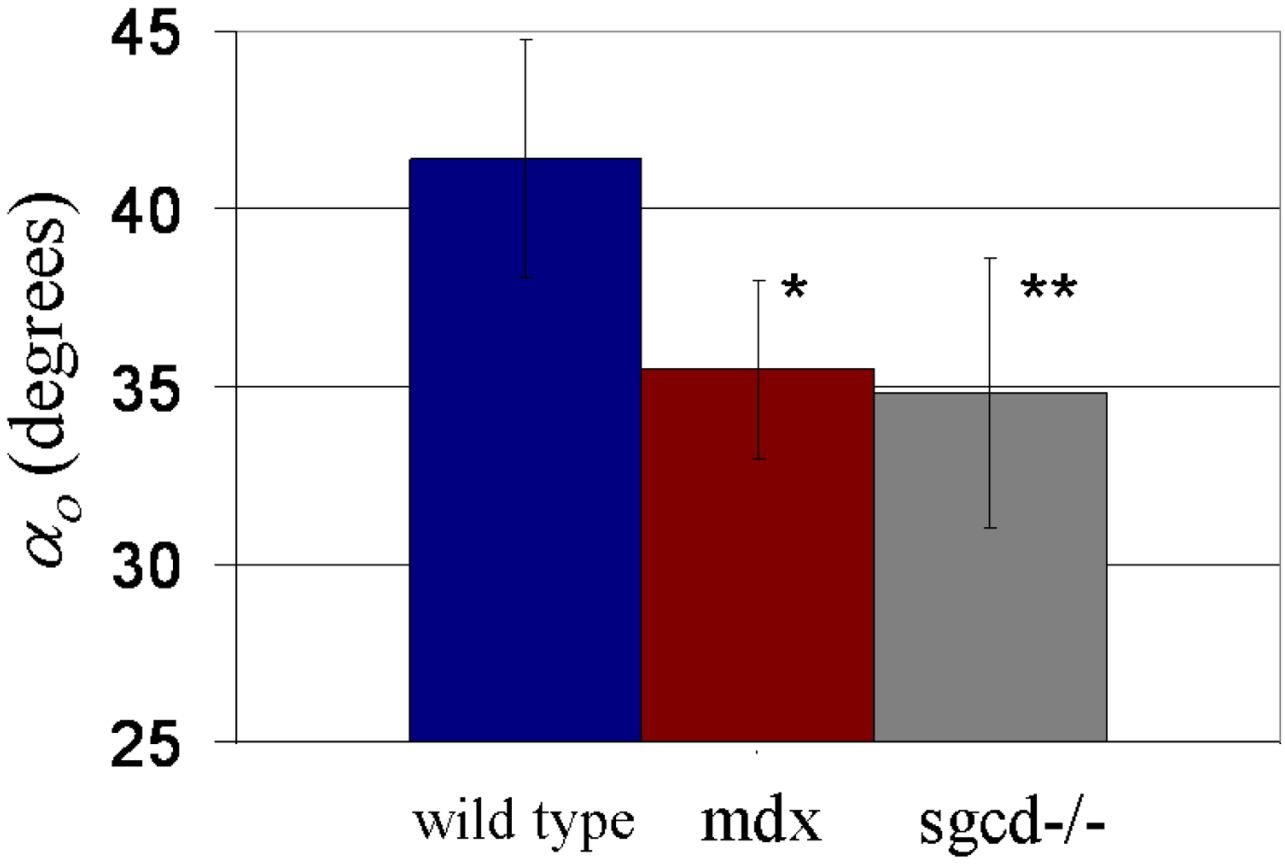

Figure 2.

Mean ± S.D. of best-fit fiber angles ($\alpha_o^3 = -\alpha_o^4 = \alpha_o$) determined via nonlinear regression for wild-type, mdx, and sgcd−/− common carotid arteries. Note: * ($p = 0.013$) and ** ($p = 0.056$) indicate the level of statistical significance when compared to wild-type vessels as determined by a paired *t*-test.

Table 1

Material parameters, error, and strain energy calculated for in vivo loading conditions for the Chuong and Fung (1986) model. Material parameters were determined via a nonlinear least squares regression with mechanical testing data collected from wild-type, mdx, and scgd−/− mouse carotid arteries. Note that the strain energy was evaluated at P = 100 mmHg and the individual in vivo stretches: λ_z = 1.84, 1.71, and 1.73 for wild-type, mdx, and sgcd−/−, respectively. Superscripts (1) indicates $p < 0.05$ when comparing mdx and sgcd−/− to wild-type, (2) indicates $p < 0.10$ when comparing mdx and sgcd−/− to wild-type, (3) indicates $p < 0.05$ when comparing mdx to sgcd−/−, and (4) indicates $p < 0.10$ when comparing mdx to sgcd−/−.

	c(kPa)	c_1	c_2	c_3	c_4	c_5	c_6	Error	W(kJ/m^3)
Wild-type									
011305	202.05	0.250	0.308	1.032	0.019	0.185	0.0181	0.323	97.0
012705	400.32	0.113	0.234	0.474	0.044	0.149	0.0414	0.236	112.9
102704	171.36	0.182	0.341	0.873	0.022	0.208	0.0000	0.287	88.8
110104	232.22	0.099	0.184	0.130	0.007	0.000	0.0000	0.332	79.3
110304	110.12	0.282	0.384	1.339	0.071	0.284	0.1892	0.349	69.1
110504	302.56	0.224	0.197	0.662	0.033	0.114	0.0743	0.306	87.4
Average	**236.44**	**0.192**	**0.275**	**0.752**	**0.033**	**0.157**	**0.0538**	**0.305**	**89.1**
+/− SD	**102.59**	**0.074**	**0.082**	**0.426**	**0.023**	**0.096**	**0.0721**	**0.040**	**15.0**
mdx									
012505	33.15	0.551	1.038	5.381	0.216	1.233	0.4372	0.364	52.3
020105	48.67	0.340	0.845	3.940	0.059	0.895	0.0000	0.339	66.1
112204	40.83	0.543	0.793	3.039	0.140	0.637	0.2681	0.302	49.7
121404	31.30	0.594	0.939	2.111	0.137	0.387	0.0000	0.312	54.0
121504	67.46	0.445	0.702	1.708	0.154	0.416	0.2408	0.277	56.1
Average	**44.28**$^{(1)}$	**0.494**$^{(1)}$	**0.864**$^{(1)}$	**3.236**$^{(1)}$	**0.141**$^{(1)}$	**0.714**$^{(1)}$	**0.1892**	**0.319**	**55.6**$^{(1)}$
+/− SD	**14.67**	**0.102**	**0.130**	**1.478**	**0.056**	**0.355**	**0.1884**	**0.034**	**6.3**
sgcd−/−									
011405	42.26	0.253	0.994	3.638	0.088	0.993	0.0749	0.322	66.5
011905	66.68	0.226	0.642	1.946	0.080	0.554	0.0000	0.307	60.2
012005	102.23	0.391	0.476	0.482	0.056	0.079	0.0000	0.330	65.3
111704	82.32	0.401	0.623	2.211	0.128	0.511	0.2073	0.285	64.7
120304	96.66	0.344	0.494	1.665	0.099	0.385	0.1156	0.275	62.1
122104	62.98	0.302	0.757	1.943	0.089	0.473	0.1192	0.281	66.4
Average	**75.52**$^{(1,3)}$	**0.319**$^{(1,3)}$	**0.664**$^{(1,3)}$	**1.981**$^{(1,4)}$	**0.090**$^{(1)}$	**0.499**$^{(1)}$	**0.0862**	**0.300**	**64.2**$^{(1)}$
+/− SD	**22.58**	**0.072**	**0.192**	**1.015**	**0.024**	**0.296**	**0.0795**	**0.023**	**2.5**

Table 2

Material parameters, error, and strain energy calculated for in vivo loading conditions for the four-fiber family model. Material parameters were determined via a nonlinear least squares regression with mechanical testing data collected from wild-type, mdx, and scgd−/− mouse carotid arteries. Note that the strain energy was evaluated at P = 100 mmHg and the individual in vivo stretches: λ_z = 1.84, 1.71, and 1.73 for wild-type, mdx, and sgcd−/−, respectively. Superscripts (1) indicates $p < 0.05$ when comparing mdx and sgcd−/− to wild-type, (2) indicates $p < 0.10$ when comparing mdx and sgcd−/− to wild-type, (3) indicates $p < 0.05$ when comparing mdx to sgcd−/−, and (4) indicates $p < 0.10$ when comparing mdx to sgcd−/−.

	$b_1 c$ (kPa)	b_2^1 (kPa)	b_3^1	b_2^2 (kPa)	b_3^2	b_2^3 (Pa)	b_3^3	α_0 (deg)	*Error*	W (kJ/m^3)
Wild-type										
011305	30.11	20.65	0.067	13.93	0.202	2.43	1.811	45.1	0.254	102.6
012705	25.93	36.35	0.019	13.32	0.104	203.87	0.834	39.0	0.180	123.1
102704	17.11	25.84	0.040	15.06	0.080	7.55	1.239	37.8	0.225	96.5
110104	11.60	24.63	0.011	7.61	0.061	0.91	1.248	41.2	0.264	83.7
110304	16.35	23.38	0.000	7.61	0.193	10.42	1.330	39.2	0.248	78.4
110504	26.39	19.32	0.038	17.48	0.183	1.14	2.171	46.3	0.226	93.1
Average	**21.58**	**25.03**	**0.029**	**12.50**	**0.137**	**37.72**	**1.439**	**41.4**	**0.233**	**96.2**
+/− SD	**7.55**	**6.06**	**0.024**	**4.05**	**0.063**	**81.49**	**0.475**	**3.5**	**0.030**	**15.8**
mdx										
012505	25.95	15.42	0.112	7.30	0.262	70.70	1.394	38.8	0.287	66.9
020105	23.11	23.11	0.052	13.78	0.131	28.40	1.184	32.3	0.258	83.7
112204	19.41	17.98	0.063	7.50	0.351	230.98	1.033	36.5	0.219	60.7
121404	12.75	20.28	0.076	19.76	0.176	1409.52	0.803	33.7	0.254	63.7
121504	11.70	23.68	0.071	15.63	0.164	1479.02	0.727	35.9	0.239	63.1
Average	**18.59**	**20.09**$^{(2)}$	**0.075**$^{(1)}$	**12.79**	**0.217**	**643.72**	**1.028**	**35.5**$^{(1)}$	**0.251**	**67.6**$^{(1)}$
+/− SD	**6.26**	**3.48**	**0.022**	**5.38**	**0.089**	**735.10**	**0.273**	**2.5**	**0.025**	**9.2**
***sgcd*−/−**										
011405	10.89	31.49	0.037	10.63	0.071	130.43	0.890	30.4	0.239	82.6
011905	13.62	25.94	0.000	11.39	0.082	243.40	0.764	31.6	0.234	73.1
012005	21.76	30.23	0.040	12.62	0.339	106.45	1.369	40.6	0.253	77.5
111704	23.79	23.73	0.049	14.51	0.184	272.28	0.993	36.3	0.226	77.5
120304	21.24	20.95	0.024	14.16	0.181	568.35	0.761	36.7	0.211	72.7
122104	12.44	28.69	0.062	9.25	0.142	705.84	0.719	33.2	0.227	76.1
Average	**17.29**	**26.84**	**0.035**$^{(3)}$	**12.09**	**0.167**	**337.79**$^{(1)}$	**0.916**$^{(1)}$	**34.8 (2)**	**0.232**	**76.6**$^{(1)}$
+/− SD	**5.58**	**4.04**	**0.021**	**2.06**	**0.097**	**244.27**	**0.244**	**3.8**	**0.014**	**3.6**

Table 3

Material parameters for the Rachev and Hayashi (1999) model determined via a nonlinear least squares regression with mechanical testing data collected from wild-type, mdx, and scgd−/− mouse carotid arteries under basal tone. Note that the best-fit parameters for the four-fiber family model (Table 2) were used to model the passive mechanical behavior. No significant differences were observed for T_{act}, λ_M, and λ_o across any groups.

	t_{act} (kPa)	λ_M	λ_o	*Error*
Wild-type				
011305	21.5	1.71	0.90	0.244
012705	12.6	1.80	0.91	0.187
102704	11.7	1.81	0.91	0.646
110104	7.6	1.86	0.93	0.280
110304	14.6	1.78	0.92	0.184
110504	23.8	1.74	0.89	0.190
Average	**15.3**	**1.78**	**0.91**	**0.289**
+/− **SD**	**6.2**	**0.05**	**0.02**	**0.179**
mdx				
012505	17.6	1.73	0.90	0.267
020105	14.8	1.80	0.92	0.358
112204	13.8	1.79	0.92	0.329
121404	13.2	1.82	0.92	0.337
121504	9.6	1.84	0.92	0.244
Average	**13.8**	**1.79**	**0.91**	**0.307**
+/− **SD**	**2.9**	**0.04**	**0.01**	**0.049**
sgcd−/−				
011405	18.7	1.70	0.89	0.280
011905	8.7	1.84	0.92	0.252
012005	23.6	1.75	0.89	0.243
111704	23.3	1.77	0.87	0.265
120304	8.4	1.84	0.92	0.230
122104	13.8	1.79	0.92	0.288
Average	**16.1**	**1.78**	**0.90**	**0.260**
+/− **SD**	**6.8**	**0.06**	**0.02**	**0.022**